Dalton Transactions

Helicity inversion and redox chemistry of chiral manganese(II) cubanes

Journal:	*Dalton Transactions*
Manuscript ID:	DT-ART-05-2014-001590.R1
Article Type:	Paper
Date Submitted by the Author:	02-Jul-2014
Complete List of Authors:	Deville, Claire; University of Geneva, Department of Inorganic and Analytical Chemistry Granelli, Matteo; University of Geneva, Department of Inorganic and Analytical Chemistry Downward, Alan; University of Geneva, Department of Inorganic and Analytical Chemistry Besnard, Céline; University of Geneva, Laboratory for X-ray Crystallography Guénée, Laure; University of Geneva, Laboratory for X-ray Crystallography Williams, Alan; University of Geneva, Dept of Inorganic and Analytical Chemistry

Graphical abstract

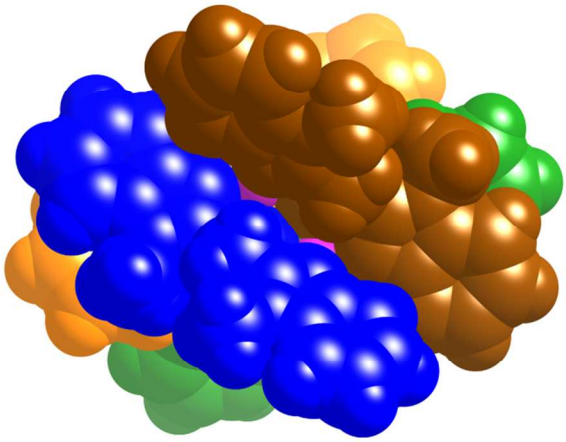

N-Methylation of a benzimidazole ligand switches the helicity of a tetranuclear manganese complex and changes the redox behavior.

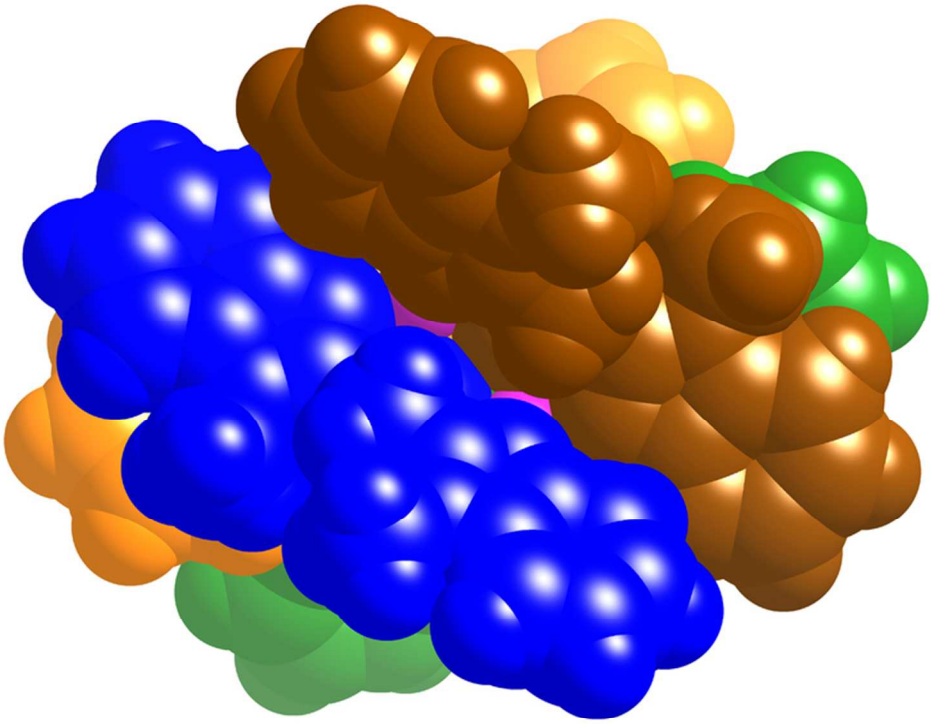

71x63mm (300 x 300 DPI)

Journal Name

RSCPublishing

ARTICLE

Helicity inversion and redox chemistry of chiral manganese(II) cubanes

Cite this: DOI: 10.1039/x0xx00000x

Claire Deville,[a] Matteo Granelli,[a] Alan M. Downward,[a] Céline Besnard,[b] Laure Guenée[b] and Alan F. Williams[a,*]

Received ooth January 2012,
Accepted ooth January 2012

DOI: 10.1039/x0xx00000x

www.rsc.org/

The chiral ligand *S*-1,2-bis(1*H*-benzimidazol-2-yl)ethanol, **1**, reacts with manganese(II) salts to form cubanes which readily undergo oxidation reactions leading either to a tetranuclear manganese(II,III) mixed valence complex **4** or to a tetranuclear complex of ligand **5** where the secondary alcohol has been oxidised to an enolate. N-methylation of ligand **1** slows the oxidation reaction and stable manganese(II) cubanes may be isolated. The fully methylated ligand **2** gives a cubane of opposite helicity to that found previously for **1** with cobalt. The inversion may be explained by conformational analysis. Cyclic voltammetry suggests that the manganese cubanes reported here are insufficiently robust to store oxidising equivalents as in the oxygen evolving system of photosystem II.

Introduction

Transition metal cubanes containing a core M_4X_4 unit (Scheme 1) have for long attracted the attention of coordination chemists as examples of self-assembled tetranuclear species. The cubanes of manganese where M = Mn and X is an oxygen ligand (typically oxo-, hydroxo-, or alkoxo-) have been of particular interest in recent years. They show a remarkable range of oxidation states, ranging from $[Mn(I)_4]$ to $[Mn(IV)_4]$, corresponding to a change of 12 electrons.[1] The oxygen evolving centre (OEC) of photosystem II was for many years thought to involve a manganese cubane, although the most recent structural determination seems to confirm that it in fact contains a hetero- $CaMn_3$ cubane with a fourth manganese closely associated,[2] and there have been a number of recent attempts to synthesise such heterocubanes and study the effect of the calcium ion on the redox chemistry of the manganese.[3-5] However Mn_4 cubanes are generally more accessible synthetically and have been studied to give further understanding of the chemistry of manganese in the OEC,[6-8] and also in connection with the general question of catalysis of oxygen evolution[9] where cobalt cubanes have been shown to be active. The cubane structure allows significant magnetic exchange between metal ions and manganese cubanes have been studied for their magnetic properties, particularly in the search for single molecule magnets.[10-14]

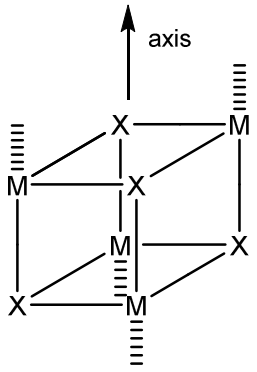

Scheme 1. Schematic view of a cubane. The axis around which the ligands twist is shown, together with the binding sites of the bridging ligands (as hatched lines).

We recently reported that the readily prepared chiral ligand *S*-1,2-bis(1*H*-benzimidazol-2-yl)ethanol, **1** forms cubanes with cobalt(II) in which four ligands twist around an axis corresponding to one of the four-fold axes of the cube (Scheme1).[15] The alcohol oxygen is deprotonated and occupies the X site. The benzimidazole groups bind to the metal coordination sites perpendicular to the axis. The octahedral coordination of the metal ion is completed by complexation along the axis of two further ligands such as a carboxylate or diphenylphosphinate (DPP^-) which bridge the two metal ions on the face of the cube. We were therefore interested to see firstly whether similar cubanes can be generated with

manganese and secondly whether there is an interesting redox chemistry associated with such cubanes.

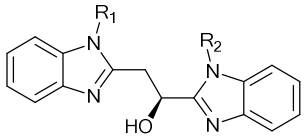

$R_1 = R_2 = H$: *S*-**1**
$R_1 = R_2 = Me$: *S*-**2**
$R_1 = Me, R_2 = H$: *S*-**3**

Scheme 2. Ligands used in this work

Apart from the ligand **1** which we studied previously,[15] we have also studied ligands **2** and **3** where the pyrollic hydrogen of the benzimidazole is replaced completely (**2**) or partially (**3**) by a methyl group. It is well known from previous work using benzimidazoles that the dissociable proton can couple with redox processes at the metal[16-20] and methylation can prevent this.[21] However, alkylation at the nitrogen also affects the conformation of the ligand[22] and it therefore seemed interesting to see if this modified the binding of the ligand to the cubane. Finally we show that aryl carboxylates can replace the DPP^- anion and undergo intramolecular stacking interactions.

Results

Synthesis

Ligand *S*-**2** was prepared in a similar way to ligand *S*-**1** from L-(-)malic acid and *N*-methyl-1,2,-benzene diamine. Ligand *S*-**3** was prepared from *S*-3-(1*H*-Benzimidazol-2-yl)-3-hydroxypropanoic acid[23] by a Philips reaction[24] with *N*-methyl-1,2,-benzene diamine.

The complexes were prepared in a manner analogous to the cobalt complexes by mixing one equivalent of ligand and manganese(II) salt with a half equivalent of the ligand chosen for the axial site. Sufficient triethylamine was added to deprotonate the alcohol functions and the axial ligands. With ligand **1** darkening of the solution was observed immediately after the addition of base suggesting oxidation. ESI-MS shows the initial solution to contain cubanes as shown by the base peak $[Mn_4(S\text{-}\mathbf{1}\text{-}H)_4\text{-}H]ClO_4^{2+}$. When no axial ligand was present, dark red crystals were obtained by vapour diffusion of ether into the brown acetonitrile solution. X-ray crystallography (see below) showed these to be $[Mn_4(S\text{-}\mathbf{1}\text{-}H)_4(OH)_2(MeCN)_2](ClO_4)_4.MeCN(EtOH)_2$, **4**, containing two Mn(II) and two Mn(III) ions. If diphenylphosphinate (DPP^-) was present, the solution changed from brown to yellow after about two weeks, and orange crystals of $[Mn_4(\mathbf{5}\text{-}H)_4(DPP)_2](DPP)_2.5EtOH$, **6**, were obtained, containing the oxidised ligand **5** as a coordinated enolate.

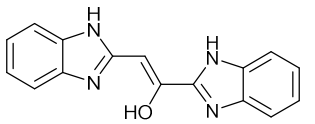

5

Scheme 3. The oxidised ligand **5**.

Ligand **5** has been reported previously as formed by dehydration of the diol ligand 1,2-bis(1*H*-benzimidazol-2-yl)ethane-1,2-diol during a hydrothermal synthesis,[25] but this is the first report of it being formed by oxidation of **1**.

The UV-visible spectra of solutions of **4** and **6** show significant differences.(Fig. S1) **4** shows strong band around 380nm (ε = 17000) which we attribute to ligand to manganese(III) charge transfer, with a significant shoulder around 500 attributed to d-d transitions. In **6** there is no manganese(III) and no d-d shoulder is observed, but there is a very strong structured absorption centred at 370 nm. This cannot be a charge transfer band, and we attribute it to a ligand-centred band at low energy resulting from the fact that the two benzimidazole units in **5** are now conjugated. This is supported by ZINDO calculations of the UV-visible spectra of **1** and **5** using the Scigress package[26] which predict a strong band at 370 nm for **5** which is absent in **1**. The CD spectrum of **4** shows a strong positive signal at 370 nm, but that of **6** is flat, as would be expected from the absence of an asymmetric carbon in the ligand (Fig. S2).

ESI-MS spectra of solutions of **4** do not show the mixed valence species but only signals typical of a manganese(II) cubane. The base peak is $[Mn_4(S\text{-}\mathbf{1}\text{-}H)_4\text{-}2H]^{2+}$. Difficulty was experienced in recording the mass spectrum of **6** which appears to decompose in the conditions of the mass spectrometer. The base peak was the protonated ligand $\mathbf{5}H^+$, followed by $DPPH_2^+$ and $[Mn_4(\mathbf{5}\text{-}H)_4\text{-}2H]^{2+}$. If the mass spectrum was recorded immediately after mixing the components, typical signals for manganese(II) cubanes such as $[Mn_4(S\text{-}\mathbf{1}\text{-}H)_4\text{-}2H]^{2+}$ were observed.

With ligand **2** no coloration was observed upon adding base, and colourless crystals of $[Mn_4(S\text{-}\mathbf{2}\text{-}H)_4(DPP)_2](ClO_4)_2$, **7** were obtained. ESI-MS showed the formation of cubanes in solution with the base peak $[Mn_4(S\text{-}\mathbf{2}\text{-}H)_4(DPP)_2]^{2+}$. The absence of oxidation tends to confirm the role of the NH protons in any redox process. With the semi-methylated ligand **3**, slight colouring of the solutions was observed, but ESI-MS showed only manganese(II) cubanes, and only manganese(II) species $[Mn_4(S\text{-}\mathbf{3}\text{-}H)_4(DPP)_2](ClO_4)_2$, **8**, and $[Mn_4(S\text{-}\mathbf{3}\text{-}H)_4(m\text{-}C_6H_4(NO_2)CO_2)_2](ClO_4)_2$, **9**, were isolated from the solutions. Their structures were determined by X-ray crystallography. ESI-MS shows that complexes of ligand **2,** which cannot dissociate a pyrrolic proton, tend to retain the axial ligand in the gas phase, whereas **1** and **3** tend to dissociate pyrrolic protons and the axial ligands.

A series of compounds with different aryl carboxylates as axial ligands, $[Mn_4(S\text{-}\mathbf{2}\text{-}H)_4(C_6H_5CO_2)_2](ClO_4)_2.3H_2O$, **10,** $[Mn_4(S\text{-}\mathbf{2}\text{-}H)_4(m\text{-}C_6H_4(NO_2)CO_2)_2](ClO_4)_2.5H_2O$, **11**, and $[Mn_4(S\text{-}\mathbf{2}\text{-}H)_4(p\text{-}C_6H_4(NO_2)CO_2)_2](ClO_4)_2.CH_2Cl_2$, **12** were prepared by a similar route. Their infrared spectra were identical to the complexes characterised structurally after allowance for the bands associated with the axial ligand (Fig. S3)

Table 1. Details of X-ray crystal structure determinations.

Compound	**4**	**6**	**7**	**8***	**9**
Formula	$C_{78}H_{83}Cl_4Mn_4N_{19}O_{24}$	$C_{122}H_{114}Mn_4N_{16}O_{17}P_4$	$C_{96}H_{89.4}Cl_2Mn_4N_{16}O_{16.7}P_2$	$C_{92}H_{80}Cl_2Mn_4N_{16}O_{16}P_2$	$C_{86}H_{76}Cl_{10}Mn_4N_{18}O_{20}$
$D_{calc.}$/ g cm^{-3}	1.426	1.347	1.439	1.297	1.600
μ/mm^{-1}	0.714	4.454	5.611	5.209	7.595
Formula Weight /g mol^{-1}	2032.19	2419.93	2087.03	2018.32	2255.90
Colour	dark red	orange	colourless	colourless	colourless
T/K	180	180	180	180	150
Wavelength	Mo Kα	Cu Kα	Cu Kα	Cu Kα	Cu Kα
Crystal System	monoclinic	monoclinic	monoclinic	trigonal	orthorhombic
Space Group	C2	C2/c	$P2_1$	$P3_221$	$P2_12_12_1$
a/Å	24.259(2)	28.4101(7)	14.444(2)	21.61754(11)	17.66452(13)
b/Å	17.5767(10)	16.1505(4)	23.205(3)	21.61754(11)	17.98233(19)
c/Å	11.3099(9)	27.3141(7)	14.665(2)	19.15394(11)	29.4766(3)
α/°	90	90	90	90	90
β/°	101.031(6)	107.760(3)	101.418(2)	90	90
γ/°	90	90	90	120	90
V/Å^3	4733.4(6)	11935.5(5)	4818.0(11)	7751.77(9)	9363.21(15)
Z	2	4	2	3	4
Θ_{min}/ Θ_{max} (°)	1.44/26.78	3.19/73.39	3.07/76.28	3.301 /72.576	3.507/72.642
Measured Refl.	22990	22646	27762	42401	39981
Independent Refl.	10030	11658	15014	10157	18189
Reflections Used	8991	9399	12201	9833	16578
R_{int}	0.0600	0.0303	0.0423	0.0253	0.0297
Parameters	567	694	1315	606	1260
Restraints	24	8	123	2	4
Largest Peak/e A^{-3}	1.194	3.414	0709	0.547	1.050
Deepest Hole/e A^{-3}	-1.625	-0.586	-0.368	-0.394	-0.967
GooF	1.239	1.086	1.001	1.061	1.043
wR_2 (all data)	0.1894	0.2335	0.1283	0.0826	0.1219
wR_2	0.1839	0.2186	0.1199	0.0814	0.1173
R_1 (all data)	0.0744	0.0851	0.0638	0.0302	0.0488
R_1	0.0672	0.0731	0.0504	0.0290	0.0441
Flack parameter	0.01(2)	-	0.02(5)	-0.005(3)	-0.005(3)

*For compound 8 a void is present in the structure, which could contain disordered solvent molecules not included in the formula. (see cif file for information)

Table 2. Mean ligand dihedral angles.

Complex	Helicity	χ_1, N(R)-C-C-C, °	χ_2, C-C-C-C, °	χ_3, C-C-C-N(R), °
$[Mn_4(S\text{-}\mathbf{2}\text{-}H)_4(DPP)_2]^{2+}$, **7**	*M*	-83.0	176.9	-125.1
$[Mn_4(S\text{-}\mathbf{3}\text{-}H)_4(DPP)_2]^{2+}$, **8**	*P*	-57.8	-176.0	-115.7
$[Co_4(S\text{-}\mathbf{1}\text{-}H)_4(DPP)_2]^{2+}$ [15]	*P*	-56.5	-166.9	-123.8
$[Mn_4(S\text{-}\mathbf{3}\text{-}H)_4(m\text{-}C_6H_4(NO_2)CO_2)_2]^{2+}$, **9**	*P*	-60.7	-176.4	-111.1
$[Mn_4(S\text{-}\mathbf{1}\text{-}H)_4(OH)_2(MeCN)_2]^{4+}$, **4,** first ligand		-60.3	65.3	113.8
4, second ligand		-34.3	179.9	-155.6
$[Mn_4(\mathbf{5}\text{-}H)_4(DPP)_2]^{4+}$, **6**		5.7	175.5	175.0

Crystal structures

Details of the crystal structure determinations are given in table 1.

Crystal structures of $[Mn_4(S\text{-}\mathbf{2}\text{-}H)_4(DPP)_2](ClO_4)_2$, 7, $[Mn_4(S\text{-}\mathbf{3}\text{-}H)_4(DPP)_2](ClO_4)_2$, 8, and $[Mn_4(S\text{-}\mathbf{3}\text{-}H)_4(m\text{-}C_6H_4(NO_2)CO_2)_2](ClO_4)_2$, 9. These compounds all show cubane structures similar to those described previously for cobalt(II)[15] in which the four bis-benzimidazol-alcohol ligands twist around the axis in a head-to-tail manner with the alcohol functions deprotonated and triply bridging. The axial ligands, DPP or *m*-nitrobenzoate, occupy axial sites on opposite faces of the cube. We were however surprised to find that in $[Mn_4(S\text{-}\mathbf{2}\text{-}H)_4(DPP)_2](ClO_4)_2$, 7, the ligand *S*-**2** adopts a *M*-helicity (Figure 1) compared with the *P*-helicity observed for cobalt(II) with *S*-**1**.[15] However, if the ligand is only partially methylated, as in $[Mn_4(S\text{-}\mathbf{3}\text{-}H)_4(DPP)_2]^{2+}$, a *P*-helicity is observed (Figure 2).

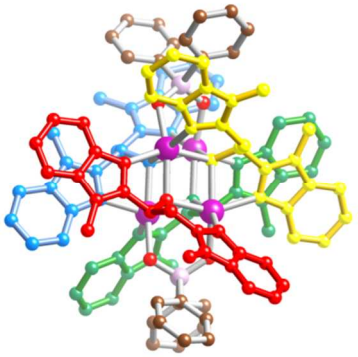

Figure 1. *M*-helicity observed for the four bridging ligands **2** in $[Mn_4(S\text{-}\mathbf{2}\text{-}H)_4(DPP)_2]^{2+}$. Hydrogens have been omitted, and the ligands colour coded. The axis of the compound is vertical

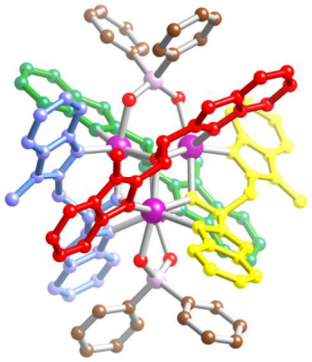

Figure 2. *P*-helicity observed for the four bridging ligands **3** in $[Mn_4(S\text{-}\mathbf{3}\text{-}H)_4(DPP)_2]^{2+}$. Hydrogens have been omitted, and the ligands colour coded.

Closer examination of the structures showed that the binding mode of the ligand **2** or **3** is slightly different in **7** and **8**. This is shown more clearly in figure 3. Both ligands bind with a five-membered and a six-membered chelate ring. In compound **8** and in the analogous cobalt complex described previously, the six-membered ring lies roughly parallel to the vertical axis in Fig. 3, while the five-membered ring is perpendicular to this axis (horizontal in Fig. 3). In **7** the five-membered ring is vertical but the six-membered ring is horizontal; this automatically flips the sense of the helicity. This may be understood by imagining rotating the ligands in Fig. 3 around the axis of the C-O bond.

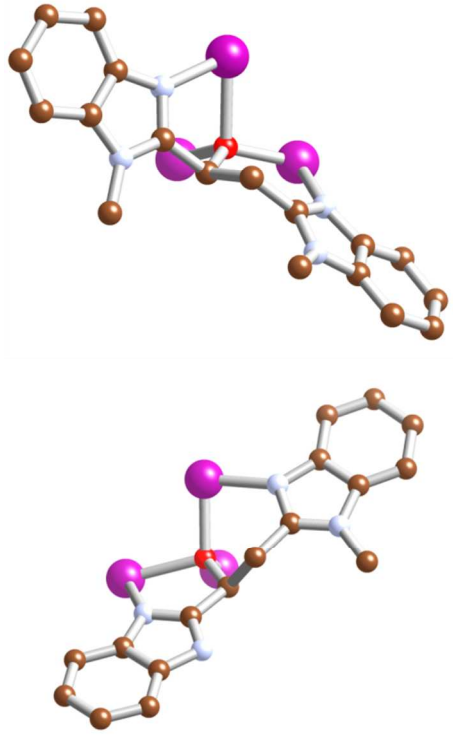

Figure 3.Comparison of the binding mode of ligands **2** and **3** in **7** (top) and **8** (bottom) respectively.

Why is the *M*-form preferred with ligand **2** and the *P*-form with ligands **1** and **3**? We have previously studied the conformation of bis-benzimidazolonium cations[22] and shown that methylation at the nitrogen atom modifies the conformation. More specifically, when R is methyl (Scheme 4) the dihedral angle χ_1 is influenced and R' influences χ_3. The greater size of the methyl group compared to hydrogen favours dihedral angles greater than 90° on methylation at nitrogen. The second dihedral angle χ_2 is generally close to 180°. The mean values of dihedral angles in the ligands are given for the complexes studied here in Table 2:

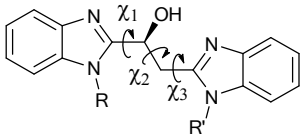

Scheme 4. Ligand dihedral angles

The values of χ_1 for the conformation giving *P*-helicity are always significantly smaller than for the conformation giving *M*-helicity. If the corresponding nitrogen is methylated, then there may be significant conformational strain. This would explain the *M*-helicity found with the fully methylated ligand **2**. For complexes of **3**, *P*-helicity is observed, but the benzimidazole involved in χ_1 is not methylated and values of the dihedral angle below 90° will be less expensive in conformational energy.

The change in helicity may thus be explained in terms of conformational effects. The metrics of the two cubanes $[Mn_4(S\text{-}\mathbf{2}\text{-}H)_4(DPP)_2]^{2+}$ and $[Mn_4(S\text{-}\mathbf{3}\text{-}H)_4(DPP)_2]^{2+}$ are otherwise very similar, both showing the common S_4^+ distortion.[27] Both show intramolecular stacking, either between benzimidazoles in neighbouring strands (two interactions) or between benzimidazoles and the aryl groups of the DPP^- ligands. The crystal packing of $[Mn_4(S\text{-}\mathbf{2}\text{-}H)_4(DPP)_2](ClO_4)_2$, **7**, shows no features of interest. In $[Mn_4(S\text{-}\mathbf{3}\text{-}H)_4(DPP)_2](ClO_4)_2$, **8**, which lies on a crystallographic two-fold axis, each ligand carries one potential hydrogen bond donor, and hydrogen bonds are observed between the four benzimidazole N-H bonds and two oxygens of the two perchlorate ions.

The compound $[Mn_4(S\text{-}\mathbf{3}\text{-}H)_4(m\text{-}C_6H_4(NO_2)CO_2)_2](ClO_4)_2$, **9** was prepared to investigate whether a change in capping anion could influence the structure. A *P*-helicity cubane is obtained, very similar to **8**. Comparison of the two $[Mn_4(S\text{-}\mathbf{3}\text{-}H)_4]^{4+}$ cores shows them to be virtually identical (Figure S4), and the conformational data are very similar. The major difference is that the capping anion can only take part in one stacking interaction, and as shown in Figure 4, it tilts to one side to maximise the interaction with one benzimidazole. Two intramolecular benzimidazole-benzimidazole stacks are present as in **8**. The crystal packing shows sheets of cations with

intermolecular stacking interactions and each perchlorate ion hydrogen bonding to two N-H bonds of neighbouring cations. The sheets are separated by dichloromethane solvent molecules.

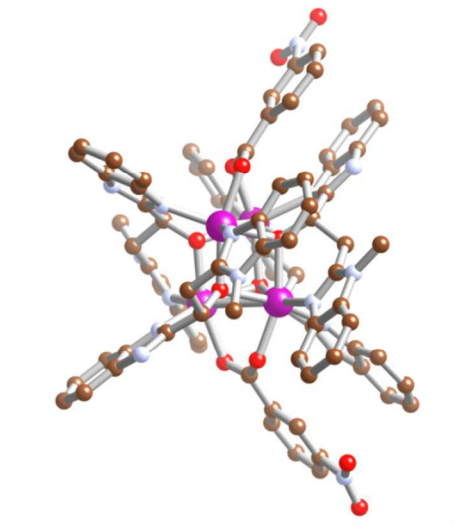

Figure 4. The cation $[Mn_4(S\text{-}\mathbf{3}\text{-}H)_4(m\text{-}C_6H_4(NO_2)CO_2)_2]^{2+}$ in **9**. The m-nitrobenzoate anion tilts away from the axis to form a strong intramolecular stack.

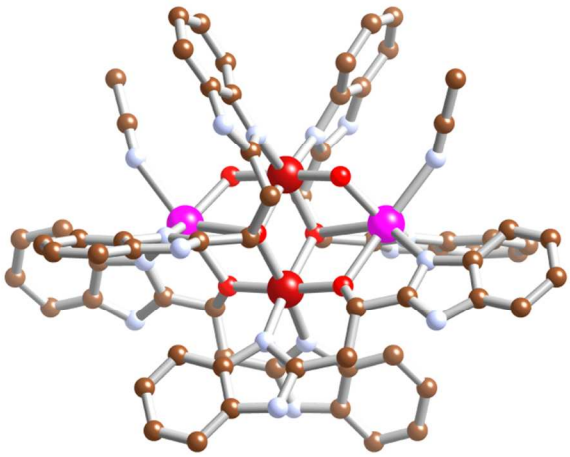

Figure 5. The structure of the cation $[Mn_4(S\text{-}\mathbf{1}\text{-}H)_4(OH)_2(MeCN)_2]^{4+}$ in **4**. Manganese(II) ions are shown as pink, manganese(III) as dark red. The two-fold symmetry axis is vertical.

Crystal structure of $[Mn_4(S\text{-}\mathbf{1}\text{-}H)_4(OH)_2(MeCN)_2](ClO_4)_4$ MeCN(EtOH)$_2$, 4. The structure of the cation in **4** is based on a lacunary double cubane, a double cube M_6O_6 from which two metal ions have been removed to give a Mn_4O_6 core. Such structures have been reported on several occasions in connection with the search for single molecule magnets.[10, 11, 28, 29] In general these cations possess a centre of inversion, but this is not possible with an enantiopure ligand such as **1**, and the cation has the crystallographic symmetry 2. The distinction between the manganese(II) and manganese(III) sites is made readily by bond valence sums[30] and by the typical Jahn-Teller distortion (two short and four long bonds) observed for the $3d^4$ Mn(III) site (Table S1). There are two crystallographically distinct ligands whose conformations are quite different (Table 1). One shows a *trans*- conformation at the central C-C bond, while the other is *gauche*. The *gauche*- ligand provides a triply bridging alkoxo- ligand, while the *trans*-ligand alkoxo- group is doubly bridging. The two OH ligands form the final pair of double bridges. The benzimidazole N-H functions and the bridging OH groups act as hydrogen bond donors to the four perchlorate ions (of which three are disordered) and the ethanol of crystallisation. The complexes stack in columns roughly perpendicular to the Mn_4 plane held together by the hydrogen bonds.

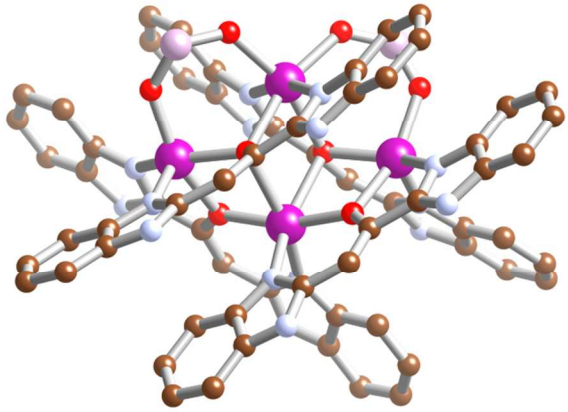

Figure 6. The cation $[Mn_4(\mathbf{5}\text{-}H)_4(DPP)_2]^{4+}$ in **6**. The two-fold axis is vertical. The aryl groups of the coordinated DPP anions have been removed for clarity.

Crystal structure of $[Mn_4(5\text{-}H)_4(DPP)_2](DPP)_2(EtOH)_5$, 6. The core of the $[Mn_4(\mathbf{5}\text{-}H)_4(DPP)_2]^{4+}$ is a Mn_4O_6 unit as in **4**, but with Mn(II) ions only. The Mn-Mn distance between the two Mn(III) ions in **4** is shorter than the equivalent distance in **6**. The oxidation of the ligand is shown by the short C-C distance and the almost planar conformation of the ligands (Table 2). The four ligands form a grid-like structure above and below the Mn_4 plane (Figure 6). The site occupied by the two bridging hydroxides in **4** is now occupied by bridging DPP^- anions in **6**. The two manganese ions on the two-fold axis have octahedral coordination, but the outer manganese ions have only five-coordination since the sixth coordination site is effectively blocked by a ligand **5**. The coordination of these manganese ions is close to square pyramidal (SP) as confirmed by the Addison τ parameter[31] of 0.15. Intramolecular stacking is observed between two ligands and one of the aryl groups of the bound DPP^- anions. In a similar way to **4** the complexes are stacked roughly perpendicular to the Mn_4 planes and held together by hydrogen bonding of the N-H functions of the benzimidazole to the uncoordinated DPP^- ions or a molecule of ethanol.

Electrochemical studies.

The synthetic results given above have shown these systems to have a varied redox chemistry, and in view of the capacity of the Mn cubane in the water oxidation centre to store oxidising equivalents, we investigated the cyclic voltammetry of some of these complexes. By taking a complex with a p-nitrobenzoate axial ligand we could use the reduction of the p-nitrobenzoate as an internal standard for current intensity. The resulting voltammogram of a solution of $[Mn_4(S\text{-}\mathbf{2}\text{-}H)_4(p\text{-}C_6H_4(NO_2)CO_2)_2]^{2+}$ is shown in Figure 7. It shows a reversible reduction peak for the p-nitrobenzoate, and irreversible oxidation at positive potentials. The oxidation begins at around +0.5 V (vs Fc^+/Fc) and a weaker reduction peak is observed on return near +0.1V. Experiments with different scan rates and multiple scans led us to conclude that decomposition occurs on oxidation with deposition of an unidentified manganese oxide on the electrode. The complexes with other aryl carboxylates or DPP^- as axial ligands showed similar behaviour.

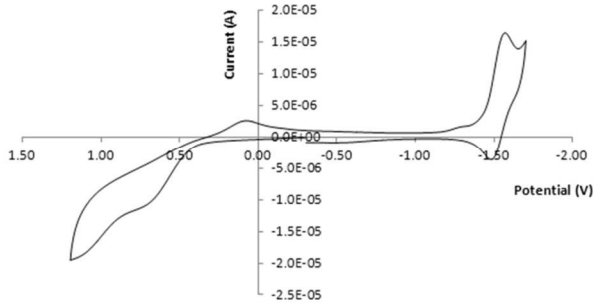

Figure 7: Cyclic voltammogram of $[Mn_4(S\text{-}\mathbf{2}\text{-}H)_4(p\text{-}C_6H_4(NO_2)CO_2)_2](ClO_4)_2.CH_2Cl_2$ in acetonitrile, referenced to ferrocene.

Conclusions

We have shown that ligand **1** and its methylated derivatives do indeed form cubanes in a manner analogous to the cobalt compounds we reported previously.[15] In contrast to the cobalt compounds, these complexes show a varied redox activity, and oxidation is generally accompanied by considerable reorganisation as shown by the structures of **4** and **6** and the irreversible nature of the cyclic voltammograms. The observation of oxidation of manganese(II) in **4** but oxidation of the ligand in **6** is at first sight surprising. However the colour changes observed suggest that the formation of **6** takes place by initial oxidation of the manganese, the Mn(III) or higher oxidation state thus formed oxidising the ligand in a second step. The pyrrolic hydrogen of the benzimidazole is clearly not entirely innocent in these redox processes since methylation of the ligand effectively stops the oxidation. We may also note that the mass spectrum of complexes of ligand **1** shows loss of these pyrrolic hydrogens.

The switching of the helicity upon *N*-methylation of the benzimidazol was surprising, but may be explained on the basis of previous observations of the effect of methylation upon conformation. Since the conformational energies are fairly small, it is possible that the difference in energy between the *P* and *M*- forms is quite small.

Experimental

General

All chemicals were obtained commercially and were used without further purification unless otherwise stated. ^{1}H NMR spectra were recorded on a Bruker Avance 400 spectrometer (400 MHz) at room temperature. Chemical shifts are given with respect to tetramethylsilane. Low resolution electrospray ionisation mass spectra were recorded on an Applied Biosystems Sciex API 150EX Ion Turbo Spray Instrument with an infusion rate of 50µL/min. Ion spray voltages: positive 5500V, negative -4500 V. Conditions for positive ions used a declustering potential of 20 V, and a focussing potential of 200V. High resolution mass spectra were obtained on a QSTAR XL (AB/MSD Sciex) instrument in an ESI positive mode by the Mass Spectrometry Laboratory, University of Geneva. Infrared spectra were obtained using a Perkin-Elmer Spectrum 1 machine fitted with a Golden Gate ATR accessory. UV-visible spectra were obtained using a Lambda 900 UV/VIS/NIR spectrometer in a 1.0 cm quartz cell. CD spectra were obtained using a JASCO J-815 spectropolarimeter in a 1.0 cm quartz cell. Electrochemical measurements were made using a BAS Epsilon instrument with a glassy carbon working electrode and platinum counter and reference electrodes in acetonitrile with NH_4PF_6 as supporting electrolyte and ferrocene as an internal standard. Microanalyses were performed at the Microchemical Laboratory of the University of Geneva.

Synthesis of ligands

Ligand **1** was prepared as described previously.[15]

Synthesis of (*S*)-1,2-Bis(*N*-methyl-benzimidazol-2-yl)ethanol, *S*-**2.** L-(-)malic acid (9.5g, 70mmol) was dissolved in 100ml HCl 4M. *N*-methyl-1,2-phenylenediamine (17.7ml, 140mmol) was added and the solution was heated at reflux for 16h. On cooling, a blue solid was formed. The solid was filtered, dissolved in ethanol/methanol 50/50 and treated with activated carbon under reflux for 4 hours. The hot solution was filtered and concentrated ammonia was added until all the product precipitated. The precipitate was filtered and recrystallised in a 50/50 ethanol/water mixture. 5.18g were obtained (yield 24%). IR (cm^{-1}) ν_{max} : 3052 (m), 2765 (br m), 1615 (w), 1505 (w), 1470 (s), 1441 (m), 1389 (m), 1332 (m), 1285 (m), 1239 (m), 1206 (w), 1120 (w), 1078 (m), 1002 (w), 937 (w), 902 (w), 862 (w), 735 (s), 676 (w), 572 (w). ^{1}H NMR (400MHz, solvent DMSO d^6, 293K, ppm): 7.63-7.48 (m, 4H, ar), 7.28-7.12 (m, 4H, ar), 6.10 (d, 1H, OH, J=6.8 Hz), 5.56 (m, 1H, CH), 3.89 (s, 3H, CH_3), 3.86 (s, 3H, CH_3), 3.70 (dd, 1H, CH_2, J=15.2, 6.0 Hz), 3.56 (dd, 1H, CH_2, J=15.2, 7.6 Hz). ES-MS (positive mode, ethanol) m/z(%): 613.7(25) $[M_2+H]^+$, 306.9(100) $[MH]^+$, 291.3(45), 289.1(50), 175.1(80), 161.3(80). Anal. Calc. for (*S*-**2**)·0.75H_2O: C 67.59%, H 6.14%, N 17.52%; Found: C 67.34%, H 5.55%, N 17.74%.

Synthesis of *S*-3-(Benzimidazol-2-yl)-3-hydroxypropanoic acid. L-(-)-malic acid (9.5 g, 71 mmol) was dissolved in 42

ml of 4 M HCl. 1,2-benzene-diamine (7.65 g, 71 mmol) was added to the mixture. The solution was refluxed during 8 hours and then left overnight at room temperature. The green crystalline solid was filtered and removed. The filtrate was cooled to 5°C and concentrated ammonia was added until the pH reached 5. The solution was left for 1 hour at 4°C. The solid was then filtered and recrystallised in a water/ethanol mixture. The microcrystalline product was filtered and dried. Yield: 30% (4.33 g). IR (cm^{-1}) ν_{max} : 3748.3 (w), 3028.6 (br s), 2984.6m (br s), 2923.1 (br s), 2865.9 (br s), 2819.9 (br s), 2764.8 (br s), 2641.8 (br m), 2518.7 (br m), 1894.8 (br w), 1634.1 (m), 1579.1 (m), 1555.0 (m), 1537.4 (m), 1515.1 (s), 1504.5 (s), 1460.7 (m), 1399.3 (s), 1377.4 (s), 1320.4 (m), 1304.9 (m), 1243.6 (w), 1223.8 (m), 1182.2 (w), 1151.6 (w), 1116.5 (w), 1097.3 (m), 1029.1 (w), 1002.5 (w), 987.1 (w), 944.6 (w), 890.4 (w), 853.4 (w), 789.5 (m), 750.3 (m), 684.6 (w), 645.1 (w), 617.1 (w), 585.6 (w), 550.8 (w), 497.4 (w). ^{1}H NMR (400MHz, solvent DMSO d^6, 293K, ppm): 12.34 (bs, 1H, acid), 7.53-7.47 (m, 2H, ar), 7.17-7.12 (m, 2H, ar), 6.04 (bs, 1H, OH), 5.17 (m, 1H, CH), 3.34 (bs, 0.5H, NH?), 2.97 (dd, 1H, CH_2, J=15.6, 5.2 Hz), 2.71 (dd, 1H, CH_2, J=15.6, 8.4 Hz). ES-MS (negative mode, ethanol) m/z(%): 433.1(15) $[M_2$-2H](Na)$^-$, 411.0(50) $[M_2$-H]$^-$, 205.1(100) [M-H]$^-$, 187.1(10).

Synthesis of *S*-1-(1*H*-benzimidazol-2-yl)2-(*N*-methyl-benzimidazol-2-yl)ethanol dihydrochloride (*S*-**3**·2HCl). In a 50 ml round bottom flask *S*-3-(Benzimidazol-2-yl)-3-hydroxypropanoic acid (1.94 g, 9.41 mmol) was dissolved in HCl 4 M (15 ml). *N*-methylbenzene-1,2-diamine (1.06 ml, 9.33 mmol) was added and the resulting solution was refluxed for 16 hours. The mixture was cooled and kept in the freezer at -30°C for 30 minutes. The green crystalline solid obtained was filtered (*S*-**3**·2HCl). Yield: 52% (1.80 g). ^{1}H-NMR (DMSO-d^6, 400 MHz, ppm): 7.98 (dd, 1H, J = 7.0, 1.4 Hz, ar), 7.85 – 7.76 (m, 3H, ar), 7.60 (pd, 2H, J = 7.3, 1.3 Hz, ar), 7.53 (dd, 2H, J = 6.1, 3.2 Hz, ar), 5.78 (dd, 1H, J = 9.1, 3.9 Hz, C<u>H</u>), 4.18 (dd, 1H, J = 15.1, 3.9 Hz, C<u>H</u>), 4.12 (s, 3H, C<u>H</u>$_3$), 3.91 (dd, 1H, J =15.1, 9.2 Hz, C<u>H</u>). Anal. Calc. for *S*-**3**·2HCl·3H_2O: C 48.70%, H 5.77%, N 13.36%; Found: C 48.66%, H 5.75%, N 13.40%.

Synthesis of *S*-1-(1*H*-benzimidazol-2-yl)2-(*N*-methyl-benzimidazol-2-yl)ethanol, *S*-***3***. *S*-**3**·2HCl (1.87 g, 4.87 mmol) was dissolved in hot MeOH + H_2O (20 + 1 ml), activated carbon was added and the mixture was refluxed for 2 hours. The solution was filtered and concentrated ammonia was added until the colour of the solution changed from dark green to bright pink. The volume of the solvent was reduced and then water was added obtaining a light orange precipitate. Yield: 45% (1.24 g). ^{1}H-NMR (DMSO-d^6, 400 MHz, ppm): 12.50 (bs, 1H, N<u>H</u>), 7.58 – 7.46 (m, 4H, ar), 7.26 – 7.07 (m, 4H, ar), 6.19 (bs, 1H, O<u>H</u>), 5.38 (dd, 1H, J = 7.4, 4.7 Hz, C<u>H</u>), 3.79 (s, 3H, C<u>H</u>$_3$), 3.64 – 3.51 (m, 1H, C<u>H</u>$_2$), 3.42 (dd, 1H, J = 15.1, 8.5 Hz, C<u>H</u>$_2$). <u>IR</u> (cm^{-1}) ν_{max}: 3030 (br, s), 1616 (w), 1591 (w), 1504 (w), 1478 (m), 1442 (s), 1405 (m), 1332 (w), 1310 (w), 1274 (m), 1239 (w), 1148 (w), 1126 (w), 1069 (m), 1033 (w), 920 (w), 903 (w), 879 (w), 843 (m), 750 (s), 667 (w), 620 (w).Anal. Calc. for *S*-3·0.25H_2O: C 68.79%, H 5.60%, N 18.87%; Found: C 68.53%, H 5.42%, N 19.04%.

Synthesis of complexes

$[Mn_4(S$-**1**-H$)_4(OH)_2(CH_3CN)_2](ClO_4)_4(Et_2O)(CH_3CN)$, **4** *S*-**1** (28 mg, 0.1 mmol) and $Mn(ClO_4)_2.6H_2O$ (37 mg, 0.1 mmol) were dissolved in 4 ml acetonitrile. Triethylamine (200 µl, 0.1 mmol) was added. The yellow solution was filtered. Slow diffusion of diethylether led after one month to the formation of prismatic brown crystals suitable for X-Ray analysis. IR (cm^{-1}) ν_{max} : 3538.5 (br, m), 3305.4 (br, s), 3050.5 (br, s), 1622.9 (w), 1596.6 (w), 1532.0 (w), 1487.0 (w), 1448.3 (s), 1383.9 (m), 1320.4 (m), 1272.3 (m), 1219.5 (w), 1193.21 (w), 1074.4 (s), 915.0 (w), 846.8 (w), 820.5 (w), 739.4 (m), 642.9 (w), 617.4 (m). UV-visible (T=22°, $3*10^{-5}$M in MeCN, l=1cm) λ_{max}/nm (ε/$dm^3mol^{-1}cm^{-1}$): 243 (sh, 57'000), 273 (69'400), 280 (67'300), 350 (sh, 15'600), 364 (18'600), 383 (18'300), 406 (11'500). CD (T=25°, $3*10^{-5}$M in MeCN, l=1cm) λ_{max}/nm (Δε): 406 (34.25), 385 (41.88), 369 (15.50). ES-MS of initial solution (positive soft mode, acetonitrile) m/z(%): 763.2(55) $[Mn_4(S$-**1**-H$)_4$-H$]ClO_4^{2+}$, 663.5(100) $[Mn_4(S$-**1**-H$)_4$-H$]^{2+}$, 332.4(70) $[Mn_4(S$-**1**-H$)_4]^{4+}$. Anal Calc for $[Mn_4(S$-**1**-H$)_4(OH)_2(CH_3CN)_2](ClO_4)_4·2(CH_3CN)·2(C_4H_{10}O)$: C 46.35%, H 4.18%, N 13.51%; Found: C 47.34%, H 3.92%, N 13.42%.

$[Mn_4($**5**-H$)_4(DPP)_2](DPP)_2(EtOH)_5$, **6** *S*-**1** (28 mg, 0.1 mmol), $Mn(ClO_4)_2.6H_2O$ (37 mg, 0.1 mmol) and diphenylphosphinic acid (21mg, 0.1mmol) were dissolved in 3ml ethanol. Triethylamine, 0.5 M in ethanol (600 µl, 0.3 mmol) and 3 ml CH_2Cl_2 were added. The yellow solution was filtered. Very slow evaporation of this solution led after two weeks to the formation of orange prismatic crystals suitable for X-Ray analysis. Replacement of ethanol by isopropanol also gave good crystals. IR (cm^{-1}) ν_{max} : 3393.4 (br, m), 3054.3 (br, s), 2892.3 (br, m), 2756.0 (br, m), 2650.5 (br, m), 1631.7 (m), 1613.9 (m), 1592.2 (m), 1538.5 (m), 1481.0 (w), 1447.5 (m), 1434.4 (m), 1403.5 (m), 1341.5 (m), 1318.2 (m), 1281.1 (m), 1228.3 (w), 1149.4 (m), (1124.9 (s), 1070.4 (w), 1043.9 (m), 1011.4 (m), 989.8 (m), 923.6 (w), 868.7 (w), 849.0 (w), 743.8 (m), 721.6 (m), 692.7 (m), 596.9 (w), 555.9 (m), 539.9 (m), 489.5 (w). UV-visible (T=22°, $3*10^{-5}$M in EtOH/CH_2Cl_2 50/50, l=1cm) λ_{max}/nm (ε/$dm^3mol^{-1}cm^{-1}$): 407 (32'500), 382 (sh, 59'000), 365 (71'500), 352 (sh, 57'000), 292 (40'500), 282 (40'500), 273 (sh, 35'500). The CD spectrum was measured but no significant signal was observed. ESI-MS (positive mode, acetonitrile + 2 drops of water) m/z(%): 659.5(50) $[Mn_4($**5**-H$)_4$-2H$]^{2+}$, 437.5(15) $[(DPPH)_2$+H$]^+$, 277.5(100) [**5**+H$]^+$, 263.5(30), 219.4(70) $[DPPH_2]^+$. Anal Calc for $[Mn_4($**5**-H$)_4(DPP)_2](DPP)_2·6H_2O$: C 58.55%, H 4.21%, N 9.75%; Found: C 58.35%, H 4.01%, N 9.65%.

$[Mn_4(S$-**2-H**$)_4(DPP)_2](ClO_4)_2$, **7.** *S*-**2** (31 mg, 0.1 mmol), $Mn(ClO_4)_2·6H_2O$ (37 mg, 0.1 mmol) and diphenylphosphinic acid (DPPH) (21 mg, 0.1 mmol) were dissolved in 3 ml ethanol. Triethylamine 0.5 M in ethanol (400 µl, 0.2 mmol) and 3 ml CH_2Cl_2 were added. The colorless solution was filtered. Very slow evaporation of this solution gives within a few days colorless crystals suitable for X-Ray analysis. IR

(cm^{-1}) ν_{max} : 3538.5 (br, w), 3054.7 (w), 2949,5 (w), 2329.7 (br, w), 1614.1 (w), 1592.2 (w), 1480.3 (m), 1451.4 (m), 1408.1 (w), 1323.1 (w), 1294.1 (w), 1265.6 (w), 1239.3 (w), 1221.7 (w), 1152.7 (m), 1125.2 (m), 1075.3 (s), 1038.2 (m), 1017.8 (m), 935.0 (w), 886.6 (w), 857.8 (w), 807.4 (w), 744.1 (m), 723.3 (m), 702.1 (w), 622.5 (w), 556.3 (m), 542.1 (w), 500.4 (w). UV-visible (T=22°, $3*10^{-5}$M in EtOH/CH_2Cl_2 50/50, l=1cm) λ_{max}/nm (ε/$dm^3mol^{-1}cm^{-1}$): 286 (48'500), 278 (44'900). The CD spectrum was measured showed no significant peak between 300 and 800 nm. ES-MS (positive soft mode, ethanol) m/z(%): 1975.4 (2) $[Mn_4(S\text{-}\mathbf{2}\text{-}H)_4(DPP)_2](ClO_4)^+$, 937.5 (100) $[Mn_4(S\text{-}\mathbf{2}\text{-}H)_4(DPP)_2]^{2+}$, 858.8(7) $[Mn_4(S\text{-}\mathbf{2}\text{-}H)_4(DPP)(AcO)]^{2+}$, 779.5(50) $[Mn_4(S\text{-}\mathbf{2}\text{-}H)_4(AcO)_2]^{2+}$, 219.1(50) $[DPPH+H]^+$. The product was contaminated by the acetate present in the mobile phase of the ES-MS spectrometer. This is the explanation for the acetate adducts observed as well as the strong peak at m/z 219.1 corresponding to the DPP bridge that was replaced by the acetate contaminant. Anal. Calc. for $[Mn_4(S\text{-}\mathbf{2}\text{-}H)_4(DPP)_2](ClO_4)_2{\cdot}4H_2O$: C 53.72%, H 4.51%, N 10.44%; Found: C 53.61%, H 4.47%, N 10.16%;

$[Mn_4(S\text{-}\mathbf{3}\text{-}H)_4(DPP)_2](ClO_4)_2$, **8**. $Mn(ClO_4)_2{\cdot}6H_2O$ (41.9 mg, 0.12 mmol), *S*-**3** (34.3 mg, 0.12 mmol) and DPPH (25.2 mg, 0.12 mmol) were dissolved in MeOH/CH_2Cl_2 = 1/1 (4 ml) to obtain a colourless solution. Et_3N (465 µl, 0.5 M in EtOH, 0.23 mmol) was added and the solution became light yellow. Slow evaporation of the solvent led to the formation of a crystalline solid. Yield: 27% (16.2 mg). IR (cm^{-1}) ν_{max}: 3290 (m), 3059 (w), 1618 (w), 1595 (w), 1480 (m), 1452 (s), 1407 (m), 1336 (w), 1274 (m), 1213 (w), 1148 (m), 1132 (m), 1069 (s), 1037 (S), 1017 (m), 922 (w), 899 (w), 873 (m), 849 (m), 727 (s), 697 (m), 653 (w), 622(m). ES-MS (soft positive mode, MeCN + one drop of DMSO) m/z: 829.7 (2) $[Mn_4(S\text{-}\mathbf{3}\text{-}H)_4(DPP)(AcO)]^{2+}$, 800.8 (3) $[Mn_4(S\text{-}\mathbf{3}\text{-}H)_4(DPP)\text{-}H]^{2+}$, 691.8 (14) $[Mn_4(S\text{-}\mathbf{3}\text{-}H)_4\text{-}2H]^{2+}$, 219.4 (100) $[DPPH+H]^+$. Anal. Calc. for $[Mn_4(S\text{-}\mathbf{3}\text{-}H)_4(DPP)_2](ClO_4)_2{\cdot}2.5H_2O$: C 53.55%, H 4.15%, N 10.86%.; Found: C 53.49%, H 4.00%, N 10.82%.

$[Mn_4(S\text{-}\mathbf{3}\text{-}H)_4(m\text{-}NO_2PhCOO)_2](ClO_4)_2(CH_2Cl_2)_4$, **9**. In a test-tube, $Mn(ClO_4)_2{\cdot}6H_2O$ (44.7 mg, 0.12 mmol), H-*S*-**3** (36.8 mg, 0.12 mmol) and sodium *m*-nitrobenzoate (23.5 mg, 0.12 mmol) were dissolved in MeOH/CH_2Cl_2 = 1/1 (4 ml) to obtain a light yellow solution. Et_3N (245 µl, 0.5 M in EtOH, 0.12 mmol) was added and the solution became light brown. Slow evaporation of the solvent, in 24 hours, led to the formation of a crystalline solid. Yield: 53% (36.8 mg). IR (cm^{-1}) ν_{max}: 3267 (br, w), 1595 (w), 1559 (w), 1535 (w), 1484 (w), 1444 (w), 1389 (w), 1302 (w), 1230 (s), 1183 (m), 1122 (br, s), 981 (s), 873 (w), 808 (w), 744 (m), 718 (m), 622 (w). ES-MS (soft positive mode, MeCN/DCM, 2:1, m/z): 1715.9 (2) $[Mn_4(S\text{-}\mathbf{3}\text{-}H)_4(m\text{-}NO_2PhCOO)_2\text{-}H]^+$, 858.2 (8) $[Mn_4(S\text{-}\mathbf{3}\text{-}H)_4(m\text{-}NO_2PhCOO)_2]^{2+}$, 691.3 (100) $[Mn_4(S\text{-}\mathbf{3}\text{-}H)_4\text{-}2H]^{2+}$. Anal. Calc. for $[Mn_4(S\text{-}\mathbf{3}\text{-}H)_4(m\text{-}NO_2PhCOO)_2](ClO_4)_2{\cdot}3H_2O$: C 49.99%, H 3.79%, N 12.80%; Found: C 49.65%, H 3.76%, N 12.85%.

$[Mn_4(S\text{-}\mathbf{2}\text{-}H)_4(PhCOO)_2](ClO_4)_2{\cdot}3H_2O$, **10.** 37 mg of $Mn(ClO_4)_2.6H_2O$ (0.1 mmol) was dissolved in 3 ml of a N_2 degassed solution of EtOH:DCM (50/50). 31 mg *S*-**2** (0.1 mmol), 12 mg benzoic acid (0.1 mmol), and 400 µl of a 0.5 M ethanolic solution of triethylamine (0.2 mmol) were dissolved in a second nitrogen degassed EtOH:DCM solution (50/50). The two solutions were combined under a nitrogen atmosphere and left to stand for 3 hours. After standing a stream of nitrogen was used to concentrate the solution by about half before being left to stand overnight. 37.9 mg of product was obtained by filtration (79%). IR (cm^{-1}) ν_{max}: 1594 (w), 1542 (m), 1485 (m), 1451 (m), 1399 (m), 1324 (w), 1295 (w), 1264 (w), 1210 (w), 1151 (w), 1068 (br, s), 1009 (w), 935 (w), 889 (w), 856 (w), 746 (s), 719 (s), 675 (w), 622 (m), 525 (br ,w), 501 (w), 427 (br, m). ES-MS (soft positive mode, MeCN): 841.3 (36) $[Mn_4(S\text{-}\mathbf{2}\text{-}H)_4(PhCOO)_2]^{2+}$, 779.5 (100) $[Mn_4(S\text{-}\mathbf{2}\text{-}H)_4(AcO)_2]^{2+}$ Anal. Calc. for $[Mn_4(S4\text{-}H)_4(PhCOO)_2](ClO_4)_2{\cdot}3H_2O$:C 53.34%, H 4.37%, N 11.57%; Found C 53.30%, H 4.46%, N 11.50%

$[Mn_4(S\text{-}\mathbf{2}\text{-}H)_4(m\text{-}NO_2PhCOO)_2](ClO_4)_2{\cdot}5H_2O$, **11**. 36.2 mg of $Mn(ClO_4)_2.6H_2O$ (0.1 mmol) was dissolved in 3 ml of a N_2 degassed solution of EtOH:DCM (50/50). 30.6 mg *S*-**2** (0.1 mmol), 18.9 mg sodium 3-nitobenzoate (0.1 mmol), and 200 µl of a 0.5 M ethanolic solution of triethylamine (0.1 mmol) were dissolved in a second nitrogen degassed EtOH:DCM solution (50/50). The two solutions were combined under a nitrogen atmosphere and left to stand for 3 hours, during which time a white precipitate started to form. After standing a stream of nitrogen was used to concentrate the solution by about half, before being left to stand for a further 2 hours. 36.6 mg of product was obtained by filtration (71%). IR (cm^{-1}) ν_{max}: 1596 (w), 1557 (w), 1524 (w), 1487 (m), 1453 (m), 1394 (m), 1346 (m), 1295 (w), 1265 (w), 1211 (w), 1070 (br, s), 1008 (w), 934 (w), 892 (w), 856 (w), 825 (w), 791 (w), 746 (s), 719 (s), 622 (m), 527 (br, m) ES-MS (soft positive mode, MeCN): 886.3 (92) $[Mn_4(S\text{-}\mathbf{2}\text{-}H)_4(p\text{-}NO_2PhCOO)_2]^{2+}$, 833.2 (4) $[Mn_4(S\text{-}\mathbf{2}\text{-}H)_4(p\text{-}NO_2PhCOO)(AcO)]^{2+}$, 779.5 (100) $[Mn_4(S\text{-}\mathbf{2}\text{-}H)_4(AcO)_2]^{2+}$, Anal. Calc. for $[Mn_4(S\text{-}\mathbf{2}\text{-}H)_4(m\text{-}NO_2PhCOO)_2](ClO_4)_2{\cdot}5H_2O$: C 50.08%, H 4.20%, N, 12.22%; Found C 49.92%, H 4.13%, N 12.23%

$[Mn_4(S\text{-}\mathbf{2}\text{-}H)_4(p\text{-}NO_2PhCOO)_2](ClO_4)_2{\cdot}CH_2Cl_2$, **12**. 111 mg of $Mn(ClO_4)_2.6H2O$ (0.3 mmol) was dissolved in 5 ml of a N_2 degassed solution of EtOH:DCM (50/50). 93 mg *S*-**2** (0.3 mmol), 51 mg 4-nitobenzoic acid (0.3 mmol), and 1.2 ml of a 0.5 M ethanolic solution of triethylamine (0.6 mmol) were dissolved in a second nitrogen degassed EtOH:DCM solution (50/50). The two solutions were combined under a nitrogen atmosphere and left to stand for 3 hours, during which time a pale yellow precipitate started to form. After standing a stream of nitrogen was used to concentrate the solution by about half, before being left to stand for a further 2 hours. 116 mg of product was obtained by filtration (75%). IR (cm^{-1}) ν_{max}: 2360 (br, w), 1614 (w), 1568 (m), 1520 (w), 1484 (m), 1451 (m), 1404 (m), 1342 (m), 1290 (w), 1264 (w), 1240 (w), 1212 (w), 1067 (br, s), 1008 (w), 933 (w), 890 (w), 856 (w), 824 (w), 799 (w), 746 (s), 725 (s), 622 (m), 518 (m), 442 (m), 428 (m). ES-MS (soft positive mode, MeCN): 886.3 (53) $[Mn_4(S\text{-}\mathbf{2}\text{-}H)_4(p\text{-}NO_2PhCOO)_2]^{2+}$, 779.5 (100) $[Mn_4(S\text{-}\mathbf{2}\text{-}H)_4(AcO)_2]^{2+}$ Anal. Calc. for $[Mn_4(S\text{-}\mathbf{2}\text{-}H)_4(p\text{-}NO_2PhCOO)_2](ClO_4)_2{\cdot}$DCM: C

50.79%, H 3.82%, N 12.26%; Found C 50.48%, H 3.93%, N 12.23%

X-ray crystallography.

Details of the crystal structures are summarised in Table 1. Full details of each structure are given in the .cif files available as supplementary material.

Acknowledgements

We gratefully thank the Swiss National Science Foundation for their support of this work.

Notes and references

[a] *Department of Inorganic and Analytical Chemistry, University of Geneva, 30 quai Ernest Ansermet, CH 1211 Geneva 4, Switzerland. Fax:++ 41 22 379 6830; Tel: :++ 41 22 379 6830; E-mail: Alan.Willliams@unige.ch*
[b] *Laboratory for X-ray Crystallography, University of Geneva, 24 quai Ernest Ansermet, CH 1211 Geneva 4, Switzerland*

† Electronic Supplementary Information (ESI) available: UV-visible spectra of compounds **4** and **6,** CD spectra of compounds **4** and **6,** IR-spectra for Mn_4(S-**2**-H)$_4$ cubanes with various capping ligands, Comparison of $[Mn_4(S\text{-}\mathbf{3}\text{-H})_4]^{4+}$ cores in **8** and **9**. Bond distances in $[Mn_4(\mathbf{1}\text{-H})_4(OH)_2(MeCN)_2](ClO_4)_4$ $MeCN(EtOH)_2$, **4**, Hydrogen Bonds. CCDC reference numbers 1003579-1003583. For ESI and crystallographic data in .CIF format see DOI: 10.1039/b000000x//

1. A. F. Williams, *Dalton Trans.*, 2008, 818-821.
2. Y. Umena, K. Kawakami, J.-R. Shen and N. Kamiya, *Nature*, 2011, **473**, 55-60.
3. J. S. Kanady, E. Y. Tsui, M. W. Day and T. Agapie, *Science* 2011, **333**, 733-736.
4. E. Y. Tsui and T. Agapie, *Proc. Natl. Acad. Sci. U. S. A.*, 2013, **110**, 10084-10088, S10084/10081-S10084/10086.
5. S. Mukherjee, J. A. Stull, J. Yano, T. C. Stamatatos, K. Pringouri, T. A. Stich, K. A. Abboud, R. D. Britt, V. K. Yachandra and G. Christou, *Proc. Natl. Acad. Sci. U. S. A.*, 2012, **109**, 2257-2262.
6. G. C. Dismukes, R. Brimblecombe, G. A. N. Felton, R. S. Pryadun, J. E. Sheats, L. Spiccia and G. F. Swiegers, *Acc. Chem. Res.*, 2009, **42**, 1935-1943.
7. S. Wang, H.-L. Tsai, E. Libby, K. Folting, W. E. Streib, D. N. Hendrickson and G. Christou, *Inorg. Chem.*, 1996, **35**, 7578-7589.
8. C. A. Ohlin, R. Brimblecombe, L. Spiccia and W. H. Casey, *Dalton Trans.*, 2009, 5278-5280.
9. X. Liu and F. Wang, *Coord. Chem. Rev.*, 2012, **256**, 1115-1136.
10. J. Yoo, E. K. Brechin, A. Yamaguchi, M. Nakano, J. C. Huffman, A. L. Maniero, L.-C. Brunel, K. Awaga, H. Ishimoto, G. Christou and D. N. Hendrickson, *Inorg. Chem.*, 2000, **39**, 3615-3623.
11. H. Miyasaka, K. Nakata, L. Lecren, C. Coulon, Y. Nakazawa, T. Fujisaki, K.-i. Sugiura, M. Yamashita and R. Clérac, *J. Am. Chem. Soc.*, 2006, **128**, 3770-3783.
12. C. J. Milios, A. Prescimone, A. Mishra, S. Parsons, W. Wernsdorfer, G. Christou, S. P. Perlepes and E. K. Brechin, *Chem. Comm.*, 2007, 153-155.
13. C. C. Beedle, C. J. Stephenson, K. J. Heroux, W. Wernsdorfer and D. N. Hendrickson, *Inorg. Chem.*, 2008, **47**, 10798-10800.
14. G. Karotsis, S. J. Teat, W. Wernsdorfer, S. Piligkos, S. J. Dalgarno and E. K. Brechin, *Angew. Chem. Int. Ed.*, 2009, **48**, 8285-8288.
15. C. Deville, A. Spyratou, P. Aguirre-Etcheverry, C. Besnard and A. F. Williams, *Inorg. Chem.*, 2012, **51**, 8667-8669.
16. M. Haga, *Inorg. Chim. Acta*, 1983, **75**, 29-35.
17. M. Haga, M. M. Ali and R. Arakawa, *Angew. Chem. Int. Ed. Engl.*, 1996, **35**, 76-78.
18. M. Haga, M. M. Ali, S. Koseki, K. Fujimoto, A. Yoshimura, K. Nozaki and T. Ohno, *Inorg. Chem.*, 1996, **35**, 3335-3347.
19. M. Haga, T. Ano, K. Kano and S. Yamabe, *Inorg. Chem.*, 1991, **30**, 3843-3849.
20. X. Xiaoming, M. Haga, T. Matsumura-Inoue, Y. Ru, A. W. Addison and K. Kano, *J. Chem. Soc. Dalton Trans.*, 1993, 2477-2483.
21. C. Piguet, G. Bernardinelli and A. F. Williams, *Inorg. Chem.*, 1989, **28**, 2920-2925.
22. A. Kübel-Pollak, C. J. Matthews, S. Verdan, B. Bocquet, X. Melich, A. F. Williams, F. Lavergnat, P.-Y. Morgantini and G. Bernardinelli, *New J. Chem.*, 2006, **30**, 851-860.
23. F. Delval, A. Spyratou, S. Verdan, G. Bernardinelli and A. F. Williams, *New J. Chem.*, 2008, **32**, 1394-1402.
24. M. A. Phillips, *J. Chem. Soc.*, 1928, 172-177.
25. Y.-L. Zhou, F.-Y. Meng, J. Zhang, M.-H. Zeng and H. Liang, *Crystal Growth & Design*, 2009, **9**, 1402-1410.
26. Scigress Explorer Ultra Version 7.7.0.47, Fujitsu FQS Poland, Kraków, 2007.
27. K. Isele, F. Gigon, A. F. Williams, G. Bernardinelli, P. Franz and S. Decurtins, *Dalton Trans.*, 2007, 332-341.
28. L. Lecren, Y.-G. Li, W. Wernsdorfer, O. Roubeau, H. Miyasaka and R. Clérac, *Inorg. Chem. Comm.*, 2005, **8**, 626-630.
29. L. Lecren, O. Roubeau, C. Coulon, Y.-G. Li, X. F. Le Goff, W. Wernsdorfer, H. Miyasaka and R. Clérac, *J. Am. Chem. Soc.*, 2005, **127**, 17353-17363.
30. W. Liu and H. H. Thorp, *Inorg. Chem.*, 1993, **32**, 4102-4105.
31. A. W. Addison, T. N. Rao, J. Reedijk, J. Van Rijn and G. C. Verschoor, *J. Chem. Soc. Dalton Trans.*, 1984, 1349-1356.